Solar Energy Materials & Solar Cells 144 (2016) 652–656

Contents lists available at ScienceDirect

Solar Energy Materials & Solar Cells

journal homepage: www.elsevier.com/locate/solmat

Improved chemical stability of ITO transparent anodes with a SnO_2 buffer layer for organic solar cells

Shihui Yu [a,*], Wenhao Yang [a], Lingxia Li [b], Weifeng Zhang [a,*]

[a] Key Laboratory of Photovoltaic Materials of Henan Province and School of Physics and Electronics, Henan University, Kaifeng 475004, PR China
[b] School of Electronic and Information Engineering, Tianjin University, Tianjin 300072, PR China

ARTICLE INFO

Article history:
Received 21 July 2015
Received in revised form
30 September 2015
Accepted 6 October 2015
Available online 27 October 2015

Keywords:
ITO
SnO_2
Acid treatment
Conductive oxide
Organic solar cells

ABSTRACT

The ITO transparent anode with a SnO_2 layer (SnO_2/ITO) serving as a buffer layer between the PEDOT: PSS has been prepared onto glass substrates. X-ray diffraction (XRD) shows that the SnO_2 layer exhibits an amorphous structure. After the acid treatment, the resistivity of SnO_2/ITO anodes was smaller than that of the acid-treated ITO anodes. Furthermore, the mechanism of the enhanced chemical stability by the SnO_2 buffer layer is proposed. Such SnO_2/ITO transparent anodes were used for organic solar cells (OSCs). The power conversion efficiencies (PCE) of OSCs used SnO_2/ITO anodes with a SnO_2 buffer layer thickness of 10 nm increased by 15% compared with the reference OSC used a bare ITO anode.

1. Introduction

Organic solar cells (OSCs) are a promising candidate for the next generation solar cells because of their attractive characteristics such as low cost, light weight, and mechanical flexibility [1–5]. However, low efficiency of OSCs is the major problem for their commercialization and applications. In the past few years, several methods, such as annealing treatment, adding metal nanoparticles and introducing buffer layers, have been used to improve the performance of OSCs [6–11]. In their opinion, the charge transport is an important factor to affect the device performance [12–14]. In conventional devices, poly (3, 4-ethylenedioxythiophene): poly (styrene-suffocate) (PEDOT: PSS) thin layer is often used as a buffer layer between anode and the photoactive charge generating layer. Nevertheless, PEDOT: PSS exhibited strong acidity of pH 1.5–2.5 [15,16]. As we all know, the indium tin oxide (ITO) has poor chemical stability under the environment of strong acidity and moderate acidity [17–19]. Therefore, the electrical conductivity of ITO transparent anode will deteriorate when it contacts with PEDOT: PSS. The degradation of ITO conductivity results in the destruction of its charge collection properties and transport ability, thereby decreasing the power conversion efficiency (PCE) of OSCs [20]. In order to achieve a higher efficiency of the OSCs, metal oxide buffer layer was used as anodes of OSCs to minimize chemical damage of ITO transparent anode [21]. In this work, the SnO_2 buffer layer with thicknesses of 5–15 nm was deposited on the top of ITO transparent anodes. The acid-proof investigation of the ITO and SnO_2/ITO anodes were conducted. After acid treatment, the electrical properties of ITO anode deteriorate greatly, but that of the SnO_2/ITO anodes change little. The SnO_2/ITO transparent anodes were used for of OSCs, it is shown that the short current density and the PCE of OSCs were improved.

2. Experimental

2.1. SnO_2 layer deposition

SnO_2 buffer layers with different thicknesses of 5–15 nm were deposited onto ITO transparent anodes by RF magnetron sputtering. The ceramic target was prepared by SnO_2 powder (pure 99.9%). The RF magnetron sputtering chamber was initially pumped down to 5×10^{-4} Pa. The substrates temperature, working power and Ar/O_2 gas ratio were controlled at 500 °C, 40 W and 20:1, respectively.

2.2. Characterization of SnO_2/ITO transparent anode

The crystallinity was determined by X-ray diffraction using a (XRD DX–2700, Fangyuan) system equipped with a Cu-Kα radiation source (1.542 Å) operating at 40 kV and 25 mA scanning the

* Corresponding authors. Tel./fax: +86 378 3880696.
E-mail addresses: ysh728@126.com (S. Yu), wfzhang6@126.com (W. Zhang).

http://dx.doi.org/10.1016/j.solmat.2015.10.005
0927-0248/

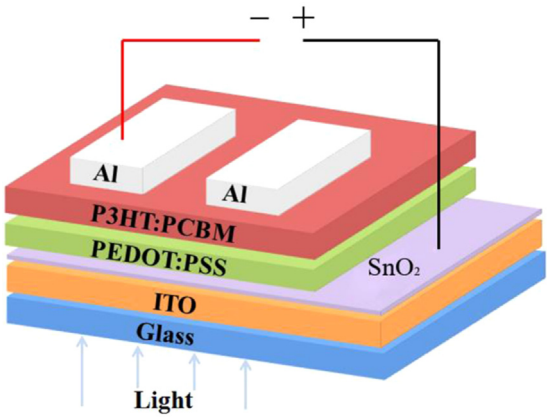

Fig. 1. A typical device structure of an OSC with SnO_2/ITO anodes.

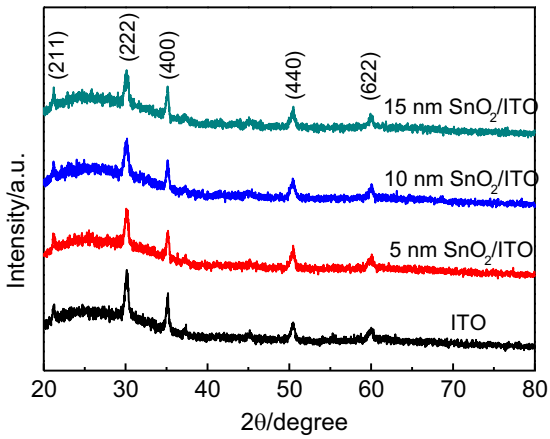

Fig. 2. XRD patterns of SnO_2/ITO anodes with SnO_2 layer thicknesses of 0–15 nm.

diffraction angles (2θ) between 20° and 80° (increment 0.02°). The AFM imaging was performed using a Nanoscope Multimode 8 (Bruker, Santa Barbara, CA, USA). The thickness of the SnO_2 layer was measured by Alpha-Step D-100 profilometer (KLA-Tencor, California, USA). Electrical properties were examined using the four-point probe technique and Hall-effect measurements (HSM 3000, Ecopia). Optical transmittance spectra were obtained on an ultraviolet–visible–near infrared (UV–Vis–NIR) spectrophotometer (Varian Cary 5000) in the wavelength range 300–800 nm.

2.3. Fabrication of OSCs

Fig. 1 illustrates the configuration of OSCs in this study, which has a structure of ITO (180 nm)/SnO_2(x nm)/PEDOT: PSS (50 nm)/P3HT: PCBM (120 nm)/Al (100 nm). The thicknesses of SnO_2 buffer layers varied from 0 to 15 nm. The PEDOT: PSS layer of ~50 nm thickness was prepared by spin coating on SnO_2/ITO anodes, and then annealed at 120 °C for 30 min on a hot-plate. The active layers (P3HT: PCBM = 1: 0.8 in the solvent of 1, 2–dichlorobenzene) were spin-coated on the PEDOT: PSS layers at 1200 rpm for 60 s in an argon-filled glove box. The P3HT (dispersion index: 2.0–2.4, average molecular weight: ~50 k, metal content is approximately 50 ppm) was purchased from Rieke Metals, Inc., PCBM from Solenne BV, the Netherlands. Then, an Al thin film as cathode was evaporated on the top of the active layer. Finally, the devices were annealed at 150 °C for 10 min in vacuum oven. The active area of device, defined by shadow mask, was 0.12 cm^2. Current density–voltage characteristics were measured using a computer-controlled Keithley 2440 under 100 mW/cm^2 simulated AM 1.5 G filters simulator. The electrical measurements of the devices were performed in air without encapsulation at room temperature.

3. Results and discussions

3.1. Characterization of the SnO_2/ITO anodes

Fig. 2 shows the XRD patterns of the SnO_2/ITO transparent anodes. The thicknesses of SnO_2 buffer layer varied from 0 to 15 nm. A broad peak due to the amorphous nature of the glass substrate can be found between 15° and 35°. It can be seen that all the thin films show planes corresponding to (2 1 1), (2 2 2), (4 0 0), (4 4 0) and (622) at 21.50°, 30.50°, 35.47°, 51.04° and 60.68°, respectively. Which are related to the crystalline structure of a cubic In_2O_3 phase [22,23]. No crystalline peaks of SnO_2 are observed which indicates that SnO_2 buffer layer exhibits an amorphous structure [24,25]. The intensities of the characteristic diffraction peaks of ITO cubic structure decrease with the increasing SnO_2 layer thickness, which can be attributed to the amorphous structure of the SnO_2 layer.

In order to intuitive observation the surface morphology of ITO thin films with different SnO_2 layer thickness, the AFM was used. Fig. 3 shows the AFM micrographs of ITO thin films with different SnO_2 layer thickness. It is clearly shown that the surface morphology changed with increasing SnO_2 thickness. At a SnO_2 thickness of 5 nm in Fig. 3a, nucleation process has completed and nucleus growth has already proceeded and island structure was appeared, disconnected SnO_2 islands appeared. These disconnected SnO_2 islands on the bottom ITO films might increase the sheet resistance and light absorption. For the 10 nm thick SnO_2 thin film, as shown in Fig. 3b, the islands connected to each other and a coalescence phenomenon was observed, a continuous Ag film was formed on the bottom ITO film. Finally, the Ag SnO_2 film with a thickness of 15 nm completely covers the bottom ITO film, as shown in Fig. 3c.

Transmission spectra of the deposited SnO_2/ITO anodes were presented in Fig. 4. It can be seen that the average transmittance in the visible range (from 380 nm to 780 nm) is 94.94%, 94.12%, 91.43%, and 91.05% of the SnO_2 buffer layer thicknesses of 0 nm, 5 nm, 10 nm and 15 nm, respectively. It is noticed that the average transmittance decreases with the increasing SnO_2 buffer layer thickness. However, the average transmittance value of all the anodes is still above 90%, which is sufficiently high for being used as anodes in the OSCs.

In order to understand the possible influence of acid PEDOT: PSS on the transparent anodes, an acid treatment on ITO and SnO_2/ITO anodes were conducted. In the acid treatment process, every samples were placed into the acid solution (PH 2.0) of a mixture of deionized water, HCl and HNO_3 (1: 1: 0.06) for 30 min. Table 1 shows the carrier concentration (n), Hall mobility (μ) and resistivity (ρ) of the ITO and SnO_2/ITO anodes before and after the acid treatment. Before the acid treatment, the carrier concentration of SnO_2/ITO anodes are slightly smaller than that of ITO anodes, and the Hall mobility and electrical resistivity of SnO_2/ITO anodes are slightly larger than that of ITO anodes. This result is attributed to amorphous SnO_2 layer. However, after the acid treatment, the carrier concentration and Hall mobility of SnO_2/ITO anodes are larger than that of ITO anodes, and the value of electrical resistivity of SnO_2/ITO anodes are smaller than that of ITO anodes. The acid treatment makes the SnO_2/ITO anodes have highly conducting compared to the same acid treated ITO anodes. Therefore, it is expected that the SnO_2/ITO anode has better electrical properties than ITO anode under the acid PEDOT: PSS than ITO anodes.

The schematic drawing in Fig. 5 shows the mechanism of the improved chemical stability of ITO transparent anodes with the